

## MRI of herpes simplex encephalitis

Ph. Demaerel<sup>1</sup>, G. Wilms<sup>1</sup>, W. Robberecht<sup>2</sup>, K. Johannik<sup>1</sup>, P. Van Hecke<sup>1</sup>, H. Carton<sup>2</sup>, and A. L. Baert<sup>1</sup>

Departments of <sup>1</sup> Radiology, <sup>2</sup> Neurology, University Hospitals K. U. Leuven, Leuven, Belgium

Received: 8 March 1991

**Summary.** The magnetic resonance imaging (MRI) findings in eight patients with herpes simplex meningoencephalitis were reviewed: 14 examinations were analysed. The most striking finding was high signal intensity in the temporal lobe(s) with the typical configuration known from CT. Meningeal enhancement after Gd-DTPA administration was clearly seen in four patients. Haemorrhagic changes are much better seen on MRI than on CT. When adequate motion control can be achieved, MRI becomes the examination of choice in the diagnosis and follow-up of herpes simplex encephalitis. Localized <sup>1</sup>H MR spectroscopy also proved promising in the study of neuronal loss.

**Key words:** Brain, diseases – Encephalitis – Magnetic resonance imaging

Herpes simplex virus type I (HSV) is the most common cause of viral meningoencephalitis in Europe. The clinical presentation is variable but the diagnosis can often be suspected. Definitive diagnosis is given by serology and cerebrospinal fluid (CSF) analysis, but these can remain normal until the 2nd week.

Computed tomography (CT) and magnetic resonance imaging (MRI) may contribute to early diagnosis or confirm a suspected diagnosis. As treatment is now available, radiology has an important role. It has been shown in two series that the CT appearance of herpes simplex meningoencephalitis (HSME) is rather typical [1, 2]. To our knowledge, this is the first report of large series of MRI findings in HSME.

### Materials and methods

We studied three men and five women ranging in age from 43 to 62 years. The presentation varied from minor changes in mental status to confusion and decreased level of consciousness. All patients were febrile.

The diagnosis was given by a rise in the serum antibody titre for HSV and by analysis of CSF. Cranial CT was obtained in all patients 1–2 days before an MR study at 1.5 T.

A spin-echo (SE) sequence was used to obtain axial T<sub>2</sub>-weighted and axial and/or coronal T<sub>1</sub>-weighted images before and after administration of gadolinium-diethylenetriamine-penta-acetic acid (Gd-

DTPA). All examinations were reviewed for the following criteria: localization, signal characteristics on T<sub>1</sub>- and T<sub>2</sub>-weighted images, mass effect, pattern of contrast enhancement and presence of haemorrhage. A total of 14 examinations were performed from 2–62 days after the onset of symptoms, 3 of which (20%) were inadequate due to patient motion artefacts.

Water-suppressed localized <sup>1</sup>H MR spectroscopy (MRS; STEAM method) was carried out on one patient. The SE time was 270 ms and the repetition time 3 s. A volume of interest of 3 × 3 × 3 cm<sup>3</sup> was centered on the pathological right temporal lobe, with an identical contralateral volume as control. A spectrum was obtained in 13 min, using 256 acquisitions. Ratios of metabolite concentrations were calculated from the corresponding peak intensity ratios.

### Results

The right temporal lobe was involved in three patients, the left in two; bilateral involvement was seen in three patients (Fig. 1). Frontal lobe involvement was present in two patients.

Lesions were seen in the gyrus rectus (*n* = 3), the cingulate gyrus (*n* = 2) and the internal capsule (*n* = 3) (Fig. 2), and, in one patient, in the basal ganglia (Fig. 3). The lesions appeared all hypointense on T<sub>1</sub>-weighted images and hyperintense with T<sub>2</sub>-weighting. Mass effect was seen in five patients (60%). In one patient this could not be seen, due to artefact.

Gd-DTPA was administered in seven patients, on a total of 8 occasions: a gyrus and sometimes nodular enhancement was seen in five cases (Fig. 4).

Haemorrhage, seen as hypointense and hyperintense areas on T<sub>2</sub>- and T<sub>1</sub>-weighted images respectively was present in four patients (50%) (Figs. 1, 5).

Additional findings were periventricular areas of hyperintensity in white matter (*n* = 4) and an incidental parietal arachnoid cyst (*n* = 1). Cortical atrophy and formation of cystic cavities were seen in three patients examined 50 days or more after the onset of the illness. A summary of the MRI findings is given in Table 1.

All CT studies were abnormal (*n* = 5) or highly suspicious (*n* = 3).

The MRS study (patient 5) was performed 7 weeks after the onset of symptoms (Fig. 6). Peaks which have been assigned previously to choline (Cho; 3.2 ppm), creatine (Cr; 3.0 ppm) and *N*-acetyl-aspartate (NAA,

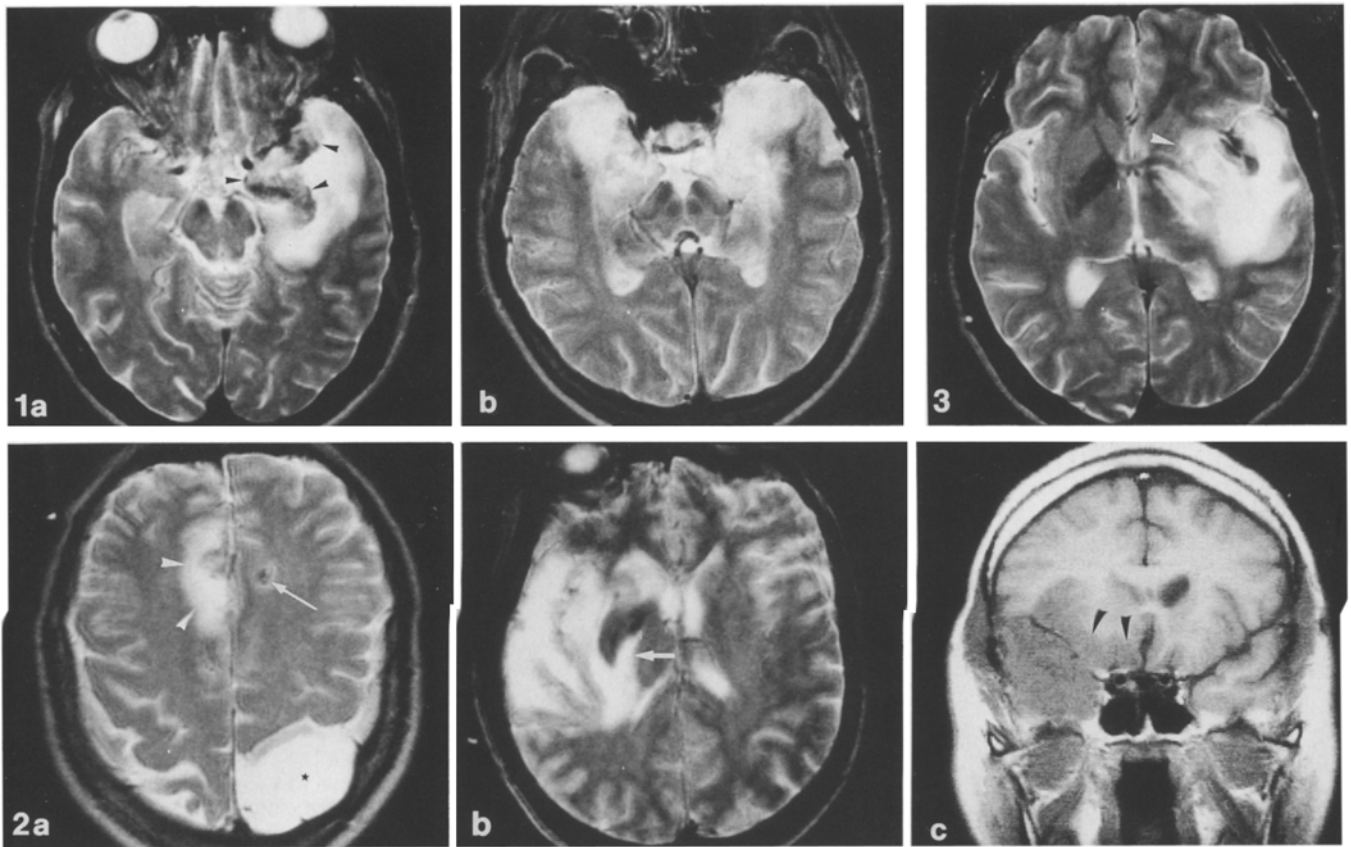


**Fig. 1.** **a** Axial T<sub>2</sub>-weighted MRI (2500/90) at 12 days after onset of symptoms shows involvement of the left temporal lobe. The hypointense area deep in the lobe (*arrows*) is presumed to be due to haemorrhagic petechial infarction. **b** Bilateral involvement of the temporal lobe on an axial T<sub>2</sub>-weighted image at 12 days in a different patient

**Fig. 2.** **a** Involvement centered on the right cingulate gyrus (*arrowheads*) on an axial T<sub>2</sub>-weighted image at 12 days. Hypointense com-

ponents probably represent haemorrhagic change (*arrow*). The arachnoid cyst (\*) was an incidental finding. **b** Involvement of the internal capsule (*arrow*) at 23 days. Coronal T<sub>1</sub>-weighted image (600/15) at 5 days shows involvement of the temporal and frontal lobe (*arrowheads*) including the gyrus rectus

**Fig. 3.** Axial T<sub>2</sub>-weighted image at 12 days shows the involvement of the lentiform nucleus (*arrowhead*). Note the sharp medial border

2.0 ppm) were observed in both spectra. A lactic acid peak (1.3 ppm) was observed in the pathological lobe; the lactate assignment was based on the spectral position at 1.3 ppm and the appearance of the characteristic doublet due to J-splitting (7.3 Hz).

The NAA/Cho and Cr/Cho ratios were calculated to be 0.71:0.50 in the pathological lobe and 1.66:0.93 in the contralateral one. The NAA/Cho value in the contralateral temporal lobe was thus still lower than the mean values found in our normal controls ( $n = 15$ ), i.e. NAA/Cho  $2.25 \pm 0.58$ , Cr/Cho  $0.95 \pm 0.17$ .

## Discussion

The early diagnosis of HSV type I meningoencephalitis is important as early institution of therapy is critical [1, 3]. The presentation is variable but should raise suspicion, and the diagnosis can be confirmed by a rise in the antibody titre for HSV type I in serum and/or in the cerebrospinal fluid [1, 2]. Most patients do not present before 5–7 days after the onset of symptoms, which can vary from minor changes in mental status to serious alterations in consciousness, leading to coma.

Pathologically, widespread haemorrhagic necrosis, with loss of all neural elements, is typically found in the inferior and medial temporal lobes. Lymphocytic infiltration of the brain and leptomeninges is seen and the presence of eosinophilic intranuclear inclusion bodies (Cowdry type A) in neurons is pathognomonic [1].

The CT appearances have repeatedly been described [1, 2].

A low density area in one or both inferomedial temporal lobes (including part of the limbic system) with extension into the insular cortex, sparing the putamen, so that the lesions have a laterally convex or straight medial border, is highly suggestive. The inferior frontal lobes, cingulate gyrus, and thalamus may be involved [1]. At some stage, but usually not before the 2nd week, meningeal contrast enhancement (CE) becomes apparent, especially around the sylvian fissure, thought to be due to a vascular proliferation adjacent to areas of necrosis, inflammation and/or petechial haemorrhagic infarctions. Residual cystic cavities may be seen. CT may be normal in the first days of the disease.

We found abnormalities on all CT studies. In three cases the findings were equivocal due to artefacts, but there was at least a high suspicion.

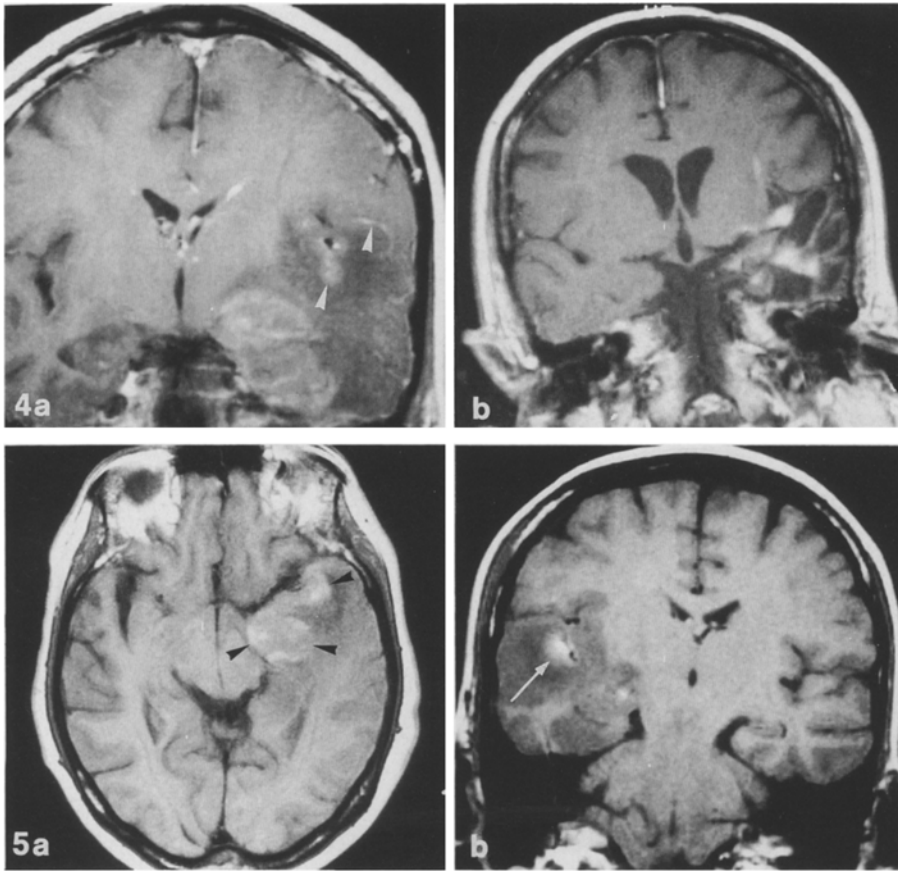


**Fig. 4.** **a** Following IV Gd-DTPA at 12 days gyral enhancement in the temporal lobe is visible (*arrowheads*) on the coronal T<sub>1</sub>-weighted image (600/15). **b** Coronal T<sub>1</sub>-weighted image at 64 days with IV Gd-DTPA shows meningeal enhancement and cystic cavities in the temporal lobe

**Fig. 5.** **a** A T<sub>1</sub>-weighted image at 12 days shows a presumed haemorrhagic component as a hyperintense area (*arrowheads*). **b** Coronal T<sub>1</sub>-weighted image at 23 days shows a hypointense lesion with some hyperintense areas (*arrow*), probably due to haemorrhage

**Table 1.** MRI in herpes simplex encephalitis

Patient age and sex	MRI (days after onset of symptoms)	Localization	Intensity on T1WI	Intensity on T2WI	Mass effect	Contrast enhancement	Haemorrhage	Remarks
1. 56, M	5	RT, GC, GR, RF	hypo	hyper	+	NA	-	Posterior internal capsule involvement
2. 62, F	21	LT	hypo (art.)	hyper (art.)	+	+	+	Early cystic cavities
	52	LT, LF	hypo	hyper	+	+	+	
3. 62, F	2	BT	hypo	hyper	+	-	-	
	56	BT	hypo	hyper	-	NA	-	
	66	BT	hypo (art.)	hyper (art.)	-	NA	-	
4. 61, F	50	BT, GR	iso/hypo	hyper	-	-	-	Residual atrophy Small cystic cavities
5. 51, F	23	RT	hypo	hyper	+	NA	+	Posterior internal capsule involvement Cystic cavities
	49	RT	hypo	hyper	+	+	+	
	64	RT	hypo	hyper	-	NA	-	
6. 53, F	5	LT	hypo (art.)	hyper (art.)	art.	NA	-	Posterior internal capsule and lentiform nucleus involvement
	12	LT	hypo	hyper	+	+	+	
7. 43, M	12	BT, GR, GC (LT > RT)	hypo	hyper	-	- (art.)	+	Arachnoid cyst in parietal lobe
8. 50, M	7	RT	hypo	hyper	+	+	-	-

art, impaired by artefact; BT, both temporal lobes; F, female; GC, cingulate gyrus; GR, gyrus rectus; hyper, hypo, iso, hyperintense, hypointense and isointense to brain; LF, LT, left frontal and temporal

lobes; M male; NA, not injected; RF, RT, right frontal and temporal lobes T1WI, T2WI, T1- and T2-weighted, images; +, present; -, absent

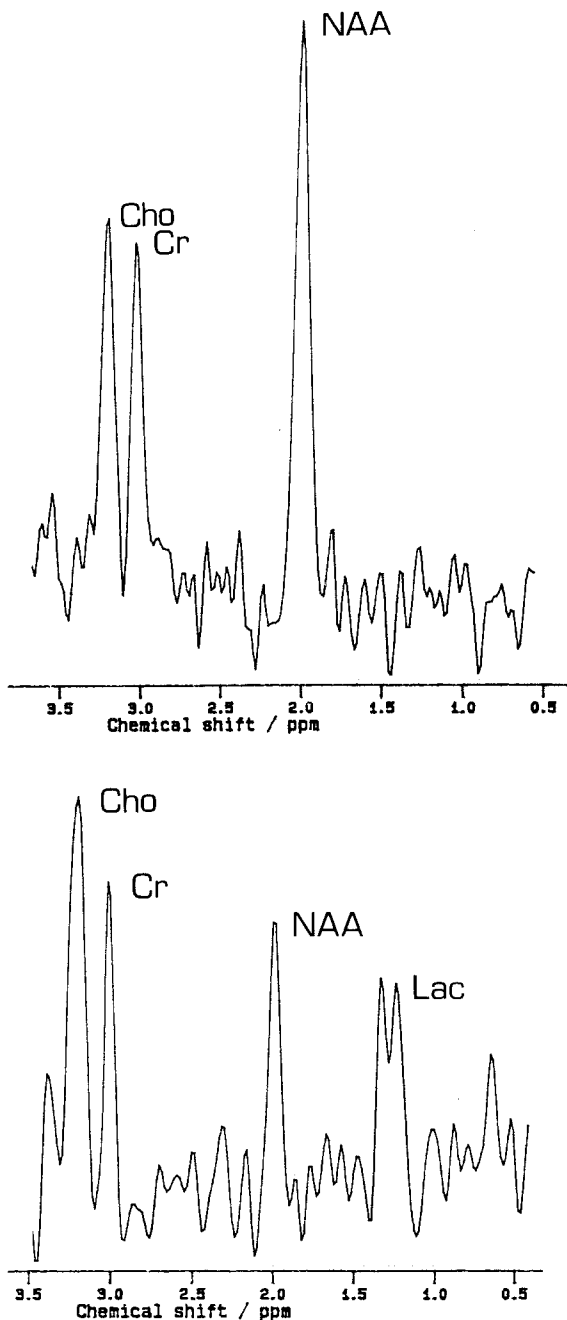


**Fig. 6.** Water-suppressed MRS at 1.5 T, using the STEAM method (TR 3 s TE 270 ms), in the left (a) and right (b) temporal lobes (VOI =  $3 \times 3 \times 3$  cm<sup>3</sup>). Peak assignments: *Cho*, choline (3.2 ppm); *Cr*, creatine (3.0 ppm); *NAA*, *N*-acetyl aspartate (2.0 ppm); *Lac*, lactic acid (1.3 ppm). Each spectrum is the sum of 256 acquisitions

It is expected that MRI, with its improved intrinsic contrast, will be superior to CT in detection and delineation of the pathological changes. von Glathe et al. [4] reported a case in which MRI showed pathological changes before CT. This could not be assessed in our series, as all patients showed abnormalities on CT, performed before MRI. The high signal intensity on T<sub>2</sub>-weighting is caused by oedema, due to inflammatory changes [4–6] (Fig. 1).

As HSV is a neurotropic virus, white matter lesions can be present [7]. The ability to obtain coronal images enables us to demonstrate clearly involvement of the island of Reil [8]. Gd-DTPA administration shows meningeal

enhancement (Fig. 4). As degradation products of haemoglobin have considerable magnetic susceptibility effect, petechial haemorrhage is much better visualized on MRI [8, 9], due to the presence of deoxyhaemoglobin and/or methaemoglobin, or to other, unknown causes of magnetic susceptibility [9] (Figs. 1, 2, 5).

Involvement of the internal capsule, the frontal lobe, and the cingulate gyrus are easily detected (Fig. 2). High signal intensity seen in the lentiform nucleus in one patient (Fig. 3) is an atypical finding.

<sup>1</sup>H MRS has proved to be a potential marker of neuronal loss; this has been shown in tumours, infarcts and recently in a case of HSME [10] (Fig. 6).

Reduction of the NAA/Cho and Cr/Cho ratios was also found in one case. The presence of a lactate peak, 7 weeks after the onset of symptoms is an atypical result, but is found in any infarct [11, 12]. An interesting finding is the decreased NAA/Cho ratio in the apparently normal hemisphere, compared to that in healthy volunteers; this may be due to metabolic changes not visible on imaging and deserves further investigation. <sup>1</sup>H MRS seems to hold promise for the future in the investigation and follow-up of HSME.

## References

- Davis JM, Davis HR, Kleinman GM, Krichner HS, Taveras JM (1978) Computed tomography of herpes simplex encephalitis, with clinicopathological correlation. *Radiology* 129: 409–417
- Enzmann DR, Ranson B, Norman D, Talberth E (1978) Computed tomography of herpes simplex encephalitis. *Radiology* 129: 419–425
- Lester JW, Warter MP, Reynolds TL (1988) Herpes encephalitis, MR monitoring of response to acyclovir therapy. *J Comput Assist Tomogr* 12: 941–943
- Glathe S von, Heindel W, Steinbrich W (1989) Die Bedeutung der Kernspintomographie in der Diagnostik zerebraler Infektionen. *Fortschr Röntgenstr* 151: 342–347
- Schroth G, Gawehn J, Thron A, Vollbracht A, Voight K (1987) Early diagnosis of herpes simplex encephalitis by MRI. *Neurology* 37: 179–183
- Davidson HD, Steiner RE (1985) MRI in infections of the cerebral nervous system. *AJNR* 6: 499–504
- Valk J, van der Knaap MS (1989) Magnetic resonance of myelin, myelination and myelin disorders. Springer, Berlin Heidelberg New York pp 244–253
- Zimmerman RA, Bilaniuk LT, Sze G (1988) Intracranial infection. In: Brant-Zawadzki M, Norman D (eds) *Magnetic resonance imaging of the central nervous system*. Raven Press, New York, pp 235–259
- Enzmann D, Chang Y, Augustyn G (1990) MR findings in neonatal herpes simplex encephalitis type II. *J Comput Assist Tomogr* 14: 453–457
- Menon DK, Sargentoni J, Peden CJ, Bell JD, Cox IJ, Coutts GA, Baudouin C, Newman CGH (1990) Proton MR spectroscopy in herpes simplex encephalitis: assessment of neuronal loss. *J Comput Assist Tomogr* 14: 449–452
- Van Rijen PC, Luyten PR, den Hollander JA, Tulleken CAF (1989) Prolonged elevation of cerebral lactate detected with <sup>1</sup>H NMR spectroscopy in patients with cerebral ischemia. *Society of Magnetic Resonance in Medicine*, Amsterdam
- Bruhn H, Frahm J, Gyngell ML, Merboldt KD, Hänicke W, Sauter R (1989) Cerebral metabolism in men after acute stroke: new observations using localized proton NMR spectroscopy. *Magn Res Med* 9: 126–131